CONTRIBUTION OF BODY TO YAWING MOMENT AND SIDEFORCE DERIVATIVES DUE TO RATE OF YAW, $(N_r)_B$ AND $(Y_r)_B$

1. NOTATION AND UNITS (see Sketch 1.1)

The derivative notation used is that proposed in ARC R&M 3562 (Hopkin, 1970) and described in Item No. 86021. Coefficients and aeronormalised derivatives are evaluated in aerodynamic body axes with origin at the aircraft centre of gravity and with the wing span as the characteristic length. The derivatives N_r and Y_r are often written as C_{nr} and C_{Yr}, and $N_{\dot{v}}$ and $Y_{\dot{v}}$ as $C_{n\dot{\beta}}$ and $C_{Y\dot{\beta}}$, in other systems of notation, but attention must be paid to the reference dimensions used. In particular, in forming C_{nr} and C_{Yr} differentiation C_n and C_Y may be carried out with respect to $rb/2V$ not rb/V as implied in the Hopkin system. Similarly $C_{n\dot{\beta}}$ and $C_{Y\dot{\beta}}$ may involve differentiation with respect to $\dot{\beta}b/2V$ not $\dot{\beta}b/V$. It is also to be noted that a constant datum value of V is employed by Hopkin.

		SI	*British*
b	wing span	m	ft
C_n	yawing moment coefficient, $\mathcal{N}/\frac{1}{2}\rho V^2 S_W b$		
C_Y	sideforce coefficient, $Y/\frac{1}{2}\rho V^2 S_W$		
d	body maximum width	m	ft
h	body maximum height	m	ft
l_b	overall body length	m	ft
l_{cg}	distance from body nose to centre of gravity position	m	ft
M	Mach number		
$\mathcal{N}$	yawing moment	N m	lbf ft
N_r	yawing moment derivative due to rate of yaw, $N_r = (\partial\mathcal{N}/\partial r)/\frac{1}{2}\rho V S_W b^2$		
$(N_r)_B$	body contribution to N_r		
$N_{\dot{v}}$	yawing moment derivative due to rate of change of sideslip, $N_{\dot{v}} = (\partial\mathcal{N}/\partial\dot{v})/\frac{1}{2}\rho S_W b^2$		
r	rate of yaw	rad/s	rad/s
S_{base}	cross-sectional area of body base	m^2	ft^2
S_b	area of side elevation of body	m^2	ft^2
S_{max}	maximum cross-sectional area of body	m^2	ft^2

S_W	wing (reference) area	m^2	ft^2
V	velocity of aircraft relative to air	m/s	ft/s
v	sideslip velocity	m/s	ft/s
$\dot{v}$	rate of change of sideslip velocity	m/s^2	ft/s^2
Y	sideforce	N	lbf
Y_r	sideforce derivative due to rate of yaw, $Y_r = (\partial Y/\partial r)/½\rho V S_W b$		
$(Y_r)_B$	body contribution to Y_r		
$Y_{\dot{v}}$	sideforce derivative due to rate of change of sideslip, $Y_{\dot{v}} = (\partial Y/\partial \dot{v})/½\rho S_W b$		
α	angle of attack	radian	radian
β	angle of sideslip	radian	radian
$\dot{\beta}$	rate of change of angle of sideslip	rad/s	rad/s
ρ	density of air	kg/m^3	$slug/ft^3$

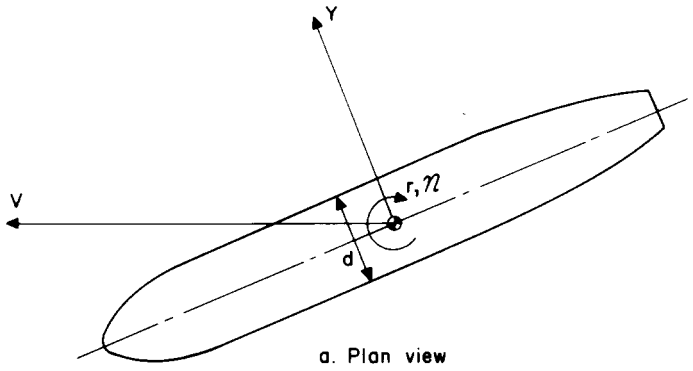

a. Plan view

◕ Centre of gravity position

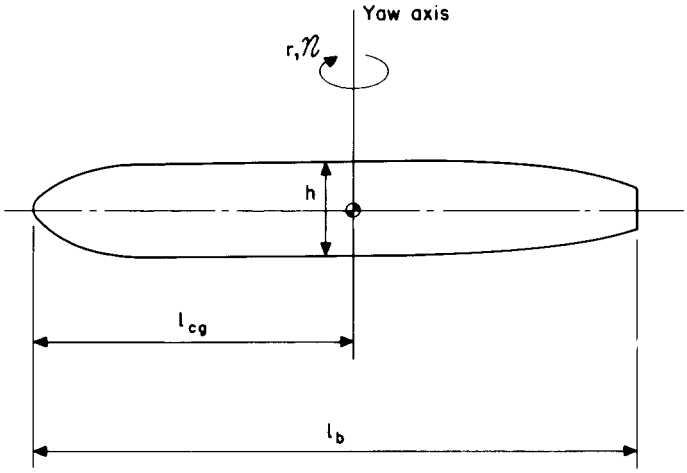

b. Side view

Sketch 1.1 Body geometry

2. INTRODUCTION

This Item provides a method for predicting the body contribution to the yawing moment derivative due to rate of yaw, $(N_r)_B$. A tentative method for predicting the body contribution to the sideforce derivative due to rate of yaw, $(Y_r)_B$, is also given, although this derivative is relatively unimportant in stability calculations. The method for $(N_r)_B$ uses the predictions of slender-body theory (Derivation 28) for bodies with finite base areas and an empirical correlation for bodies with zero base areas. The method for $(Y_r)_B$ is entirely empirical. The experimental data in Derivations 1 to 27 have been used to determine the empirical relationships and to establish the accuracy of prediction.

The method is applicable for subsonic speeds up to about $M = 0.85$ or until the aerodynamic characteristics begin to depart rapidly from their low-speed values.

Section 3 describes the method in detail, Section 4 discusses the accuracy and applicability, Section 5 gives the Derivation and References, and Section 6 gives two worked examples.

3. METHOD

3.1 General

As defined, the derivatives $(N_r)_B$ and $(Y_r)_B$ employ the wing area S_W and span b as reference dimensions in order to provide consistency with other Items dealing with stability derivatives. However, these dimensions are strictly only appropriate to the modelling of wing characteristics. Therefore, for the purposes of investigating the body derivatives the area of the side-elevation of the body S_b and the overall body length l_b have been chosen as characteristic geometric parameters for the body, these two parameters having been used successfully in Item No. 79006 (Reference 30) for modelling the body contribution to the yawing moment and sideforce derivatives due to steady sideslip. Consequently the method has been developed in terms of the parameters $(N_r)_B b^2 S_W / l_b^2 S_b$ and $(Y_r)_B b S_W / l_b S_b$, with the experimental data that have been examined being converted in the same way.

As experimental data show that the body derivatives change little with angle of attack, see Section 4.2, experimental data at zero angle of attack have been used for the purposes of comparisons. Also, in the case of the yawing moment derivative, as there are many more wind-tunnel data available from tests on wing-body configurations than there are from tests on isolated bodies, the former have been included in the analysis by estimating the contribution of the wing to N_r, using Item No. 71017 (Reference 29), and subtracting this from the experimental wing-body values. The wing contribution to N_r is small, typically in the range –0.001 to –0.005 at low values of wing lift coefficient, so this does not introduce any large errors, and the data available from those tests in which both body and wing-body data are available show that the wing-body minus wing values are a good approximation to the isolated body values. No such corrections have been applied in the case of the sideforce derivative as the wing contribution to Y_r is negligible.

Limited use has also been made of experimental data from a number of flight-tests, but the identification of the body contribution in such cases involves the subtraction of the fin contribution from the total value for the aircraft. As the fin contribution is the dominant component any errors in its estimation introduce very large uncertainties in the much smaller body contribution. Such data have therefore only been employed to confirm trends suggested by wind-tunnel test results or to investigate areas where no other data are available.

3.2 Yawing Moment Derivative

For bodies of circular cross-section shape the predictions of slender-body theory give a contribution to $(N_r)_B$ that is proportional to the product of the body base area and the square of the distance from the centre of gravity position to the base of the body (see Derivation 28 for example). This can be expressed

$$(N_r)_B b^2 S_W / l_b^2 S_b = -2(l_b - l_{cg})^2 S_{base} / l_b^2 S_b \,. \tag{3.1}$$

Figure 1 shows $(N_r)_B b^2 S_W / l_b^2 S_b$ plotted in carpet form against l_{cg}/l_b and S_{base}/S_b.

(Slender-body theory predicts an additional term that depends on the body volume multiplied by the distance between the centre of gravity position of the body and the centroid of the body volume. For practical choices of centre of gravity position that distance is small and therefore the additional yawing moment is small and has been neglected.)

Equation (3.1) has been found to give reasonable agreement with experimental data, albeit within a fairly large scatter band (see Section 4.1), for bodies with base areas greater than about 10 per cent of the maximum cross-sectional area of the body, *i.e.* $S_{base}/S_{max} > 0.1$. The equation is strictly only applicable to bodies of circular cross-section, but comparisons with experimental data suggest that the effects of cross-section shape can be ignored within the general level of accuracy of prediction. Equation (3.1) can therefore, for example, be applied to high performance military aircraft configurations that have midbody and afterbody shapes approximating to rectangular cross-sections, with body maximum height to maximum width ratios down to about $h/d = 0.35$.

For bodies with afterbodies that taper to zero base area it has been found that the mean yawing moment derivative for the available experimental data can be expressed as

$$(N_r)_B b^2 S_W / l_b^2 S_b = -0.01 \,, \tag{3.2}$$

with the predictions of this equation being of the same order of accuracy as those of Equation (3.1), (see Section 4.1). For the purposes of estimating $(N_r)_B$ for this class of bodies the position of the centre of gravity can be neglected, within the limitations of practical choice, (see Section 4.2).

The value predicted by Equation (3.2) is in apparent disagreement with Equation (3.1), which would predict a value of zero when $S_{base} = 0$, but this can be explained by supposing that the potential flow assumptions of slender-body theory break down at some point on the tapering afterbody before the end of the body is reached, giving an effective base area. The manner in which this breakdown occurs can not be predicted accurately, but comparisons of Equations (3.2) and (3.1), with $l_{cg} \approx 0.5 l_b$, suggest that it occurs so as to give an effective base area of about $0.02 S_b$. For the bodies of circular cross-section that have been studied the area $0.02 S_b$ corresponds to between 10 to 20 per cent of the body maximum cross-sectional area. For body shapes typical of light and general aviation aircraft the area $0.02 S_b$ corresponds to between 5 to 10 per cent of the body maximum cross-sectional area; (it should, however, be noted that for those aircraft there are no fin-off data with which to investigate $(N_r)_B$ directly although comparisons with flight-test data (References 22, 23 and 26) suggest that satisfactory estimates of $(N_r)_B$ are provided by Equation (3.2)).

3.3 Sideforce Derivative

Slender-body theory predicts a body contribution to Y_r that is positive and proportional to the product of the body base area and the distance from the body centre of gravity position to the body base. However, this is in poor agreement with the wind-tunnel experimental data on this derivative, which take negative values that are almost always in the range $0 > (Y_r)_B bS_W/l_b S_b > -0.08$. In view of its limited importance in terms of aircraft stability calculations, and as no method for predicting a more accurate value could be found, a simple mean value has been assumed, *i.e.*

$$(Y_r)_B bS_W/l_b S_b = -0.04\,. \tag{3.3}$$

Section 4.1.2 discusses the effectiveness of this approach.

4. ACCURACY AND APPLICABILITY

4.1 Accuracy

4.1.1 Yawing moment derivative

The overall accuracy with which $(N_r)_B b^2 S_W/l_b^2 S_b$ is predicted for the experimental wind-tunnel data in Derivations 1 to 20 is about ±0.01. This is demonstrated in Sketch 4.1 which plots experimental and predicted values of $(N_r)_B b^2 S_W/l_b^2 S_b$. The slender-body prediction of Equation (3.1) is shown in the sketch, and the data for bodies with $S_{base} = 0$ are identified at the value of –0.01 predicted by Equation (3.2).

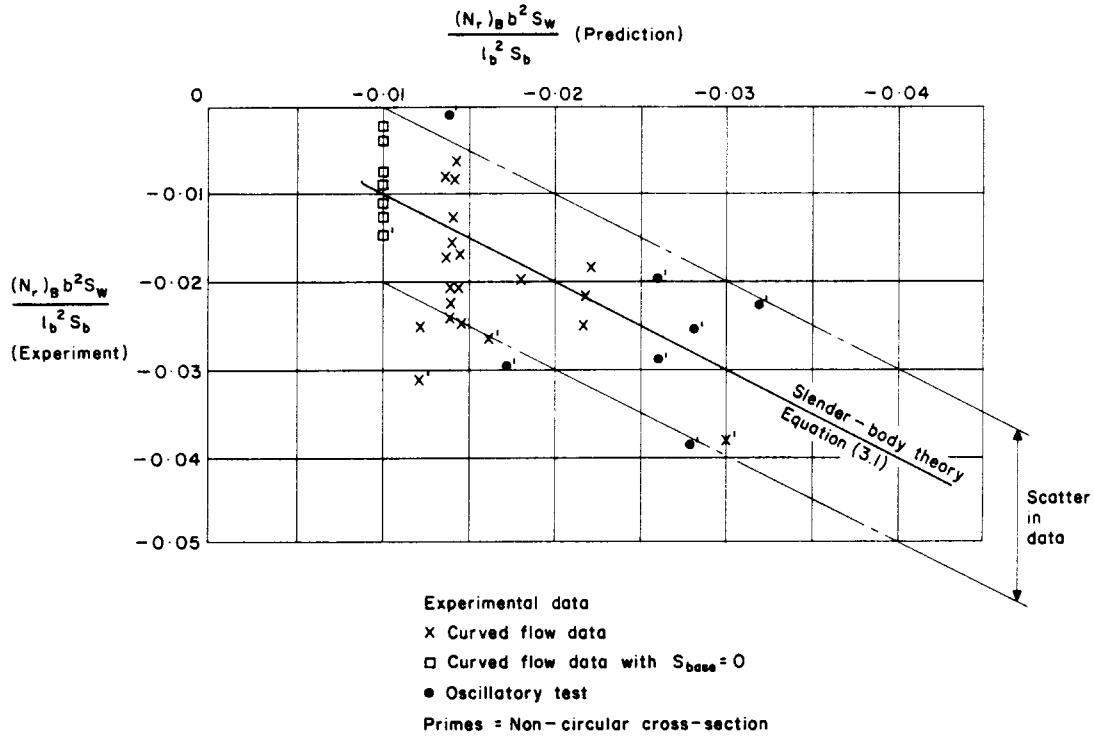

Sketch 4.1 Experimental yawing moment derivatives compared with prediction

Although the accuracy of prediction shown in Sketch 4.1 is not high it should be noted that the body contributes only about 10 to 15 per cent of the total value of N_r for an aircraft and therefore, although in itself undesirable, large percentage errors in $(N_r)_B$ are not too critical. For complete aircraft the fin provides the major contribution to N_r and Item No. 82017 (Reference 31) shows that a scatter of ± 0.02 is present in the prediction of that component. Also, the wing contribution from Item No. 71017 has a quoted accuracy of ± 0.01 . When converted to the wing reference area and span as reference dimensions the uncertainty in the prediction of $(N_r)_B$ remains within the range ± 0.01 in most cases, and therefore it is predicted to the same general level of accuracy as that to which other components of the yawing moment derivative due to yaw rate are estimated. It is also thought that the experimental data may contain a fairly high percentage scatter due to the uncertainty involved in measuring and presenting data on such a small component as $(N_r)_B$, which makes the development of a more accurate prediction method difficult.

Despite the reservations made concerning the accuracy of prediction it is considered that the method given provides a reasonable first approximation to the body contribution $(N_r)_B$. It also provides a suitable model for examining the changes in $(N_r)_B$ that may result from alterations to the fuselage of a particular aircraft such as an increase in overall length, (see Example 6.2).

When the body contribution to N_r is combined with estimates of the fin contribution from Item No. 82017 and the wing contribution from Item No. 71017, comparisons with the experimental data in Derivations 1 to 27 show that total values of N_r are predicted to within ± 0.025 in most cases at zero angle of attack. This level of accuracy is largely maintained for angles of attack up to about 15° or until separation effects on the wing or fin cause large departures from the low angle of attack values. This supports the contention that sufficiently accurate estimates of $(N_r)_B$ are being made.

4.1.2 Sideforce derivative

The overall accuracy with which $(Y_r)_B bS_W/l_b S_b$ is predicted for the experimental data in Derivations 1 to 20 is about ± 0.04 . When converted to the wing area and span as reference dimensions the uncertainty in prediction reduces slightly to ± 0.03. This is large in relation to the typical magnitude of $(Y_r)_B$ although, as in the case of the yawing moment, it is the fin that provides the major contribution to the total value for an aircraft. The accuracy quoted in Item No. 82017 for the prediction of the fin component is ± 0.04 .

When the predicted fin and body contributions are combined (the wing contribution to Y_r is negligible for attached flow), comparisons with the experimental data in Derivations 1 to 20 show that the total values of Y_r are predicted to within ± 0.05 in most cases at zero angle of attack. This level of accuracy is largely maintained for angles of attack up to about 15° or until separation effects on the wing or fin cause large departures from the low angle of attack values. In view of the fact that the effect of Y_r on the stability and control characteristics of an aircraft is small and is often neglected completely (see Derivation 3 for example) this relatively high uncertainty is not critical.

4.2 Applicability

The method assumes that there is a linear variation of yawing moment with yaw rate. Comparisons with experimental data suggest that there is little change in the magnitude of the body yaw rate derivatives with angle of attack. Data in Derivation 6 show that for an isolated body, as the angle of attack increases beyond 10° the forward part of the body can disturb the flow over the rearward part of the body so as to cause first a reduction in the magnitude of $(N_r)_B$ and eventually a change in sign. However, further data in Derivation 6 show that the presence of a wing prevents this adverse interference. Therefore, for the purposes of calculating N_r for an aircraft $(N_r)_B$ is assumed independent of angle of attack.

Almost all of the data studied were for low subsonic Mach numbers but the method should be applicable for all subsonic Mach numbers until the appearance of shock waves or flow separation effects cause a rapid

divergence from the low speed values. A few data available at high subsonic Mach numbers (Derivation 12 for example) suggest that adequate predictions are obtained for Mach numbers up to about 0.85.

The ranges of the more important geometric parameters covered in the development of the method are shown in Table 4.1. In particular note the range of l_{cg}/l_b. The values in the range 0.4 to 0.62 correspond to centre of gravity positions appropriate to civil transport and high performance military aircraft; values of about 0.35 are typical of centre of gravity positions appropriate to light and general aviation aircraft. The method should be used with caution if an untypical centre of gravity position is taken as a moment reference point.

It may also be noted that experimental data from two types of wind-tunnel test have been used, those from tests in which a curved flow is used to represent the yaw rate of the aircraft and those from tests in which the aircraft models are mounted on an oscillating rig. In the latter case the yaw rate derivatives are not measured directly but only in combination with a derivative due to the rate of change of sideslip, *i.e.* $(N_r - N_{\dot{v}})\cos\alpha$ and $(Y_r - Y_{\dot{v}})\cos\alpha$. The experimental data show that the effect of the sideslip rate derivatives on the body contribution is negligible in the case of the yawing moment, but is very important in the case of the sideforce. In particular a number of wing-body configurations, mostly of high performance military aircraft, tested on oscillating rigs showed values of $(Y_r - Y_{\dot{v}}\cos\alpha)bS_W/l_bS_b \approx +0.20$, which is very different from the prediction of Equation (3.3).

These results for oscillatory motion are in accord with slender-body theory. For $N_{\dot{v}}$, slender-body theory predicts a value for the body that is equal in magnitude but of opposite sign to the small theoretical term omitted from Equation (3.1) (see Section 3.2). Equations (3.1) and (3.2) can therefore be expected to be satisfactory for both steady yaw-rate and oscillatory motion. For $Y_{\dot{v}}$, slender-body theory predicts a value for bodies of circular cross-section that is negative and equal to twice the body volume divided by $S_W b$. Such a term is sufficiently large to account for the large positive values of $(Y_r - Y_{\dot{v}}\cos\alpha)bS_W/l_bS_b$ that have been observed in the oscillatory test data, although for bodies of irregular shape it can only be expected to give an approximate estimate. Care should therefore be taken in situations where Y_r is combined with the rate of change of sideslip derivative. (It should also be remembered that in cases where the complete aircraft is being studied in oscillatory motion, the presence of the fin, and at high angles of attack the wing, give rise to rate of change of sideslip contributions that are significant for both the yawing moment and the sideforce. (See Reference 32.))

TABLE 4.1 Ranges of Geometric Parameters

Quantity	*Range*	*Quantity*	*Range*
$l_b^2 S_b / b^2 S_W$	0.2 to 4.0	l_{cg}/l_b	0.35 to 0.62
S_{base}/S_b	0 to 0.10	h/d	0.35 to 1 a 1 to 1.25 b 1 to 1.8 c
S_{base}/S_{max}	0 and 0.1 to 0.7	l_b^2/S_b	5 to 15

a. For high performance military aircraft with ‘rectangular’ midbody and afterbody cross-section shapes.

b. For light and general aviation aircraft.

c. For aircraft with elliptical cross-sections.

5. DERIVATION AND REFERENCES

5.1 Derivation

The Derivation lists selected sources of information that have assisted in the preparation of this Item.

Wind-tunnel Data

1.	BIRD, J.D. JAQUET, B.M. COWAN, J.W.	Effect of fuselage and tail surfaces on low-speed yawing characteristics of a swept-wing model as determined in curved-flow test section of Langley stability tunnel. NACA tech. Note 2483, 1948.
2.	GOODMAN, A.	Effect of various outboard and central fins on low-speed yawing stability derivatives of a 60° delta-wing model. NACA RM L50E12a (TIL 2411), 1950.
3.	QUEIJO, M.J. GOODMAN, A.	Calculations of the dynamic lateral stability characteristics of the Douglas D-588-II airplane in high-speed flight for various wing loadings and altitudes. NACA RM L50H16a (TIL 3352), 1950.
4.	GOODMAN, A. WOLHART, W.D.	Experimental investigation of the low speed static and yawing stability characteristics of a 45° sweptback high-wing configuration with various twin vertical wing fins. NACA tech. Note 2534, 1951.
5.	FISHER, L.R. MICHAEL, W.H.	An investigation of the effect of vertical-fin location and area on low-speed lateral stability derivatives of a semitailless airplane model. NACA RM L51A19 (TIL 2655), 1951.
6.	LETKO, W.	Effect of vertical-tail area and length on the yawing stability characteristics of a model having a 45° sweptback wing. NACA tech. Note 2358, 1951.
7.	QUEIJO, M.J. WELLS, E.G.	Wind-tunnel investigation of the low-speed static and rotary stability derivatives of a 0.13-scale model of the Douglas D-558-II airplane in the landing configuration. NACA RM L52G07 (TIL 3502), 1952.
8.	BIRD, J.D. FISHER, L.R. HUBBARD, S.M.	Some effects of frequency on the contribution of a vertical tail to the free aerodynamic damping of a model oscillating in yaw. NACA Rep. 1130, 1953.
9.	FISHER, L.R. FLETCHER, H.S.	Effect of lag of sidewash on the vertical-tail contribution to oscillatory damping in yaw of airplane models. NACA tech. Note 3356, 1954.
10.	WILLIAMS, J.L.	Measured and estimated lateral static and rotary derivatives of a 1/12-scale model of a high-speed fighter airplane with unswept wings. NACA RM L53K09 (TIL 5187), 1954.
11.	JAQUET, B.M. FLETCHER, H.S.	Experimental steady-state yawing derivatives of a 60° delta-wing model as affected by changes in vertical position of the wing and in ratio of fuselage diameter to wing span. NACA tech. Note 3843, 1956.
12.	BUELL, D.A. REED, V.D. LOPEZ, A.E.	The static and dynamic-rotary stability derivatives at subsonic speeds of an airplane model with an unswept wing and a high horizontal tail. NACA RM A56I04 (TIL 6655), 1956.
13.	O'LEARY, C.O.	Transonic wind tunnel measurements of the oscillatory lateral aerodynamic derivatives of a BAC 221 model. RAE tech. Rep. 71098, 1971

14. GRAFTON, S.B. LIBBEY, C.E. — Dynamic stability derivatives of a twin-jet fighter model for angles of attack from –10° to 110°. NASA tech. Note D-6091, 1971.

15. GRAFTON, S.B. ANGLIN, E.L. — Dynamic stability derivatives at angles of attack from –5° to 90° for a variable-sweep fighter configuration with twin vertical tails. NASA tech. Note D-6909, 1972.

16. GRAFTON, S.B. CHAMBERS, J.R. — Wind-tunnel free-flight investigation of a model of a spin-resistant fighter configuration. NASA tech. Note D-7716, 1974.

17. COE, P.L. NEWSOM, W.A. — Wind-tunnel investigation to determine the low-speed yawing stability derivatives of a twin-jet fighter model at high angles of attack. NASA tech. Note D-7721, 1974.

18. O'LEARY, C.O. — Wind-tunnel measurement of lateral aerodynamic derivatives using a new oscillatory rig, with results and comparisons for the GNAT aircraft. ARC R&M 3847, 1977.

19. RAE — Unpublished wind-tunnel data from Royal Aircraft Establishment.

20. BAe — Unpublished wind-tunnel data from British Aerospace, Aircraft Group, Warton Division.

Flight-test Data

21. BIRD, J.D. JAQUET, B.M. — A study of the use of experimental stability derivatives in the calculation of the lateral disturbed motions of a swept-wing airplane and comparison with flight tests. NACA Rep.1031, 1951.

22. WOLOWICZ, C.H. YANCEY, R.B. — Lateral-directional aerodynamic characteristics of light twin-engine, propeller-driven airplanes. NASA tech. Note D-6946, 1972.

23. SUIT, W.T. — Aerodynamic parameters of the Navion airplane extracted from flight data. NASA tech. Note D-6643, 1972.

24. GILYARD, G.B. — Flight-determined derivatives and dynamic characteristics of the CV-990 airplane. NASA tech. Note D-6777, 1972.

25. SUIT, W.T. WILLIAMS, J.L. — Lateral static and dynamic aerodynamic parameters of the Kestrel aircraft (XV-6A) extracted from flight data. NASA tech. Note D-7455, 1974.

26. CANNADAY, R.L. SUIT, W.T. — Effects of control inputs on the estimation of stability and control parameters of a light aircraft. NASA tech. Paper 1043, 1977.

27. TANNER, R.R. MONTGOMERY, T.D. — Stability and control derivative estimates obtained from flight data for the Beech 99 aircraft. NASA tech. Memor. 72863, 1979.

Slender-body Theory

28. SACKS, A.H. — Aerodynamic forces, moments, and stability derivatives for slender bodies of general cross-section. NACA tech. Note 3283, 1954.

5.2 References

The References list selected sources of information supplementary to that given in this Item.

ESDU Items

29. ESDU — Aero-normalised stability derivatives: effect of wing on yawing moment due to yawing. Item No. 71017, Engineering Sciences Data Unit, London, September 1971.

30. ESDU — Wing-body yawing moment and sideforce derivatives due to sideslip: N_v and Y_v. Item No. 79006, Engineering Sciences Data Unit, London, June 1979.

31. ESDU — Contribution of fin to sideforce, yawing moment and rolling moment derivatives due to rate of yaw, $(Yr)_F$, $(N_r)_F$, $(L_r)_F$. Item No. 82017, Engineering Sciences Data Unit, London, June 1982.

Rate of Change of Sideslip Derivatives

32. COE, P.L.
GRAHAM, A.B.
CHAMBERS, J.R. — Summary of information on low-speed lateral-directional derivatives due to rate of change of sideslip $\dot{\beta}$. NASA tech. Note D-7972, 1975.

6. EXAMPLES

6.1 Example I

Calculate, for low speeds, the body contribution to the yaw rate derivatives N_r and Y_r for the configuration shown in Sketch 6.1. The wing reference area S_W is 600 ft^2 and the reference span is 63 ft. The area of the side elevation of the body is $S_b = 340$ ft^2 and the area of the base is $S_{base} = 33$ ft^2.

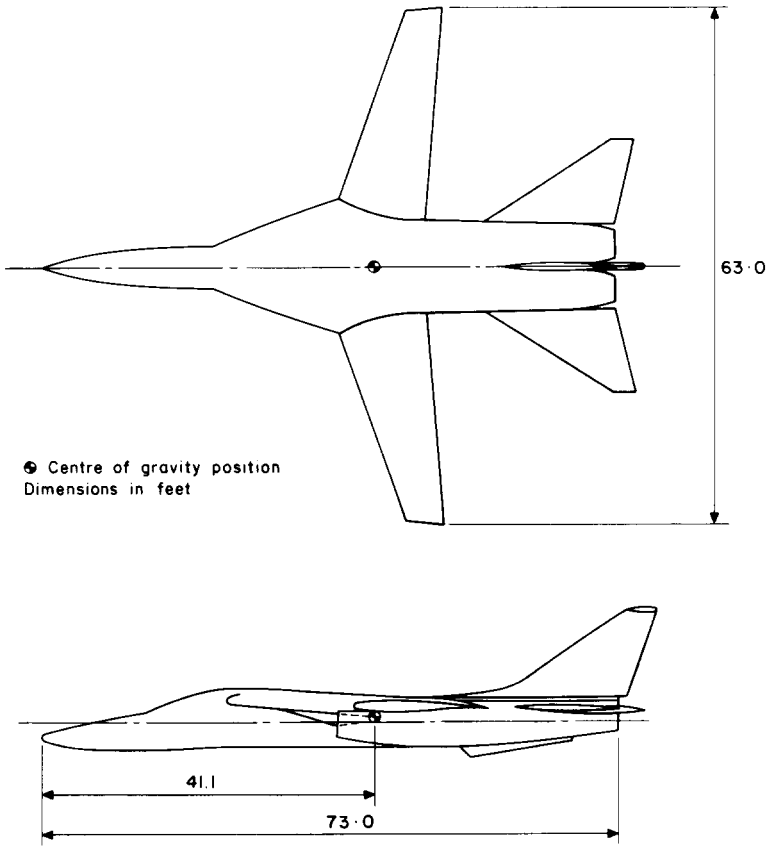

Sketch 6.1

From Sketch 6.1, $l_b = 73.0$ ft and $l_{cg} = 41.1$ ft, so that $l_{cg}/l_b = 0.563$.

From the given information $S_{base}/S_b = 0.097$.

Therefore, from Figure 1 (or Equation (3.1))

$$(N_r)_B b^2 S_W / l_b^2 S_b = -0.037,$$

and

$$(N_r)_B = -0.037 \times 73.0^2 \times 340/63^2 \times 600 = -0.028.$$

As stated in the text, Y_r is often omitted in studies of aircraft stability. If of interest, however, the body contribution may be estimated from Equation (3.3),

$$(Y_r)_B bS_W/l_b S_b = -0.040\,,$$

so that $$(Y_r)_B = -0.040 \times 73.0 \times 340/63 \times 600 = -0.026\,.$$

6.2 Example II

Calculate the change in $(N_r)_B$ caused by increasing the length of a fuselage of circular cross-section by 20 ft, as shown in side view in Sketch 6.2. The reference wing area may be taken as 1500 ft^2 and the span as 110 ft.

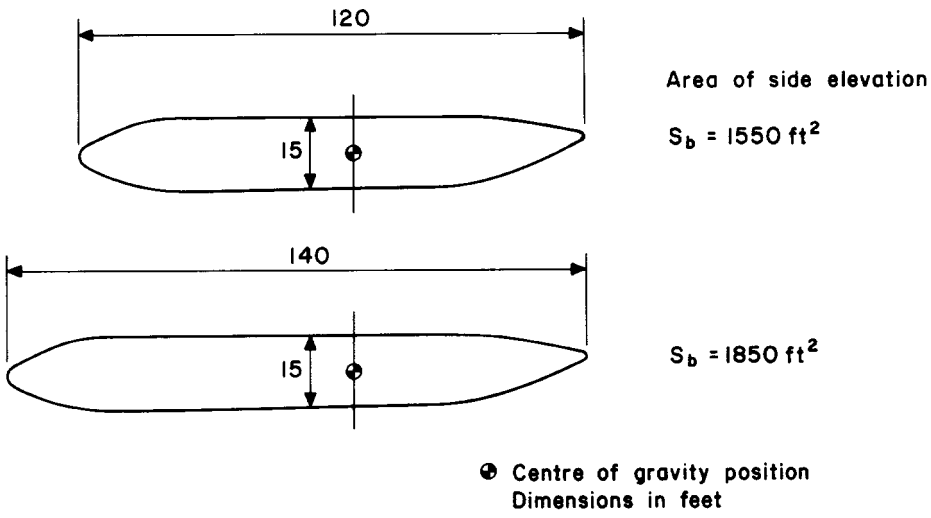

Sketch 6.2

For bodies of the type shown, which have zero base area, Equation (3.2) gives

$$(N_r)_B b^2 S_w/l_b^2 S_b = -0.01\,.$$

Therefore, for the shorter fuselage

$$(N_r)_B = -0.01 \times 120^2 \times 1550/110^2 \times 1500 = -0.012\,,$$

and for the longer fuselage

$$(N_r)_B = -0.01 \times 140^2 \times 1850/110^2 \times 1500 = -0.020\,.$$

The magnitude of $(N_r)_B$ is therefore increased by about 70 per cent because of the increase in fuselage length.

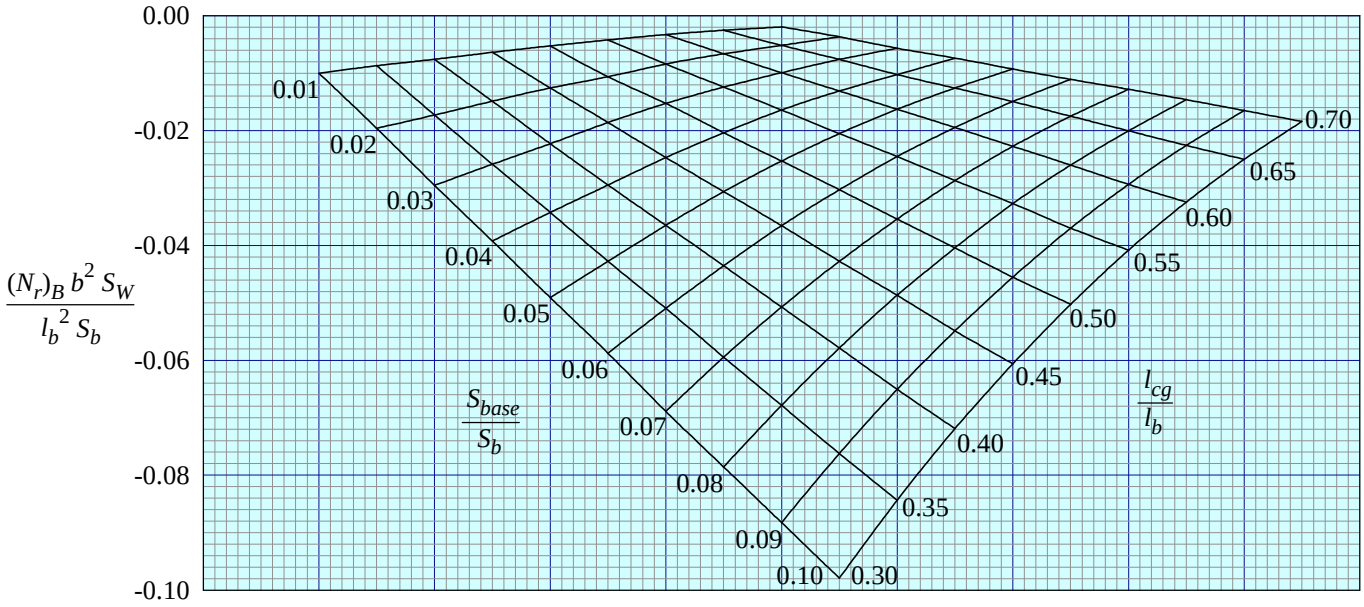

FIGURE 1 BODY YAWING MOMENT DERIVATIVE FOR $\frac{S_{base}}{S_{max}} \geq 0.1$

For bodies with Sbase = 0

$$\frac{(N_r)_B b^2 S_W}{l_b^2 S_b} = -0.01$$

(See Section 3.2)

THE PREPARATION OF THIS DATA ITEM

The work on this particular Item was monitored and guided by the Aerodynamics Committee which first met in 1942 and now has the following membership

Chairman

Mr H.C. Garner	–	Independent

Vice-Chairman

Mr P.K. Jones	–	British Aerospace, Manchester Division

Members

Mr D. Bonenfant	–	Aérospatiale, Toulouse, France
Mr E.A. Boyd	–	Cranfield Institute of Technology
Mr K. Burgin	–	Southampton University
Mr E.C. Carter	–	Aircraft Research Association
Mr J.R.J. Dovey	–	British Aerospace, Warton Division
Dr J.W. Flower	–	Bristol University
Mr A. Hipp	–	British Aerospace, Stevenage-Bristol Division
Mr J. Kloos*	–	Saab-Scania, Linköping, Sweden
Mr J.R.C. Pedersen	–	Independent
Mr I.H. Rettie*	–	Boeing Aerospace Company, Seattle, Wash., USA
Mr A.E. Sewell*	–	Northrop Corporation, Hawthorne, Calif., USA
Mr F.W. Stanhope	–	Rolls-Royce Ltd, Derby
Mr H. Vogel	–	British Aerospace, Weybridge-Bristol Division
Mr J. Weir	–	Salford University.

* Corresponding Member

The member of staff who undertook the technical work involved in the initial assessment of the available information and the construction and subsequent development of the Item was

Mr R.W. Gilbey	–	Senior Engineer.